Dense QCD: Overhauser or BCS pairing?

Byung-Yoon Park,[1,2,*] Mannque Rho,[1,3,†] Andreas Wirzba,[4,5,‡] and Ismail Zahed[1,4,§]
[1]*School of Physics, Korea Institute for Advanced Study, Seoul 130-012, Korea*
[2]*Department of Physics, Chungnam National University, Taejon 305-764, Korea*
[3]*Service de Physique Théorique, CE Saclay, 91191 Gif-sur-Yvette, France*
[4]*Department of Physics and Astronomy, SUNY-Stony Brook, New York 11794*
[5]*FZ Jülich, Institut für Kernphysik (Theorie), D-52425 Jülich, Germany*
(Received 15 October 1999; published 12 July 2000)

We discuss the Overhauser effect (particle-hole pairing) versus the BCS effect (particle-particle or hole-hole pairing) in QCD at large quark density. In weak coupling and to leading logarithm accuracy, the pairing energies can be estimated exactly. For a small number of colors, the BCS effect overtakes the Overhauser effect, while for a large number of colors the opposite takes place, in agreement with a recent renormalization group argument. In strong coupling with large pairing energies, the Overhauser effect may be dominant for any number of colors, suggesting that QCD may crystallize into an insulator at a few times nuclear matter density, a situation reminiscent of dense Skyrmions. The Overhauser effect is dominant in QCD in $1+1$ dimensions, although susceptible to quantum effects. It is sensitive to temperature in all dimensions.

PACS number(s): 12.38.Mh

I. INTRODUCTION

Quantum chromodynamics (QCD) at high density, relevant to the physics of the early universe, compact stars and relativistic heavy ion collisions, is presently attracting renewed attention from both nuclear and particle theorists. Following an early suggestion by Bailin and Love [1], it was recently stressed that at large quark density, diquarks could condense into a color superconductor [2], with potentially interesting and novel phenomena such as color-flavor locking, chiral symmetry breaking, parity violation, color-flavor anomalies, and superqualitons.

At large density, quarks at the edge of the Fermi surface interact weakly thanks to asymptotic freedom. However, the high degeneracy of the Fermi surface causes perturbation theory to fail. As a result, particles can pair and condense at the edge of the Fermi surface leading to energy gaps. Particle-particle and hole-hole pairing (BCS effect) have been extensively studied recently [1,2]. Particle-hole pairing at the opposite edges of the Fermi surface (Overhauser effect) [3] has received little attention with the exception of an early variational study by Deryagin, Grigoriev and Rubakov for a large number of colors [4], and a recent renormalization group argument in [5]. The scattering amplitude between a pair of particles at the opposite edges of the Fermi surface peaks in the forward direction, a situation reminiscent of the forward enhancement in Compton and Bhabha scattering.

In retrospect, it is surprising that the Overhauser effect in QCD has attracted so little attention. In fact, the Schwinger model [6] shows that when a uniform external charge density is applied, the electrons respond by screening the external charge and inducing a charge density wave, a situation analogous to a Wigner crystal [7–9]. Similar considerations apply to QCD in $1+1$ dimensions [8]. In $3+1$ dimensions, dense Skyrmion calculations with realistic chiral parameters yield a 3-dimensional Wigner-type crystal with half-Skyrmion symmetry at few times nuclear matter density [10,11]. At these densities, Fermi motion is expected to be overtaken by the classical interaction [12]. A close inspection of these results shows the occurrence of scalar-isoscalar, pseudoscalar-isovector and vector-isoscalar charge density waves in an ensemble of dense Skyrmions.

In this paper we will show that in dense QCD, the equations that drive the particle-hole instability at the opposite edge of a Fermi surface resemble those that drive the particle-particle or hole-hole instability in the scalar-isoscalar channel, modulo phase-space factors. In Sec. II we motivate and derive a Wilsonian action around the Fermi surface. In Sec. III we obtain expressions for the energy densities and pertinent gaps in the 0^+ channel with screening, thereby generalizing the original results in [4]. In Sec. IV, we analyze the decoupled equations for large chemical potential without screening. The effects of screening for arbitrary N_c as well as temperature are discussed in Sec. V, in overall agreement with a recent renormalization group argument [5]. In Sec. VI, we discuss the Overhauser effect in QCD in lower dimensions. Our conclusions and suggestions are given in Sec. VII. In the Appendix, we show that our simplified form of the perturbative screened gluon propagator and the exact form give the same result for the leading particle gaps.

II. EFFECTIVE ACTION AT THE FERMI SURFACE

To compare the Overhauser effect to the BCS effect, we will construct a Wilsonian effective action by integrating out the quark modes around the Fermi surface, in the presence of smooth bilocal fields. An alternative would be the quantum action [13]. At large chemical potential, most of the Fermi surface is Pauli blocked, so the quasiparticle content of the theory is well described by such an action. Incidentally, our analysis should provide a useful alternative to a brute-force lattice QCD analysis. Indeed, an effective formulation of lat-

*Email address: bypark@chaosphys.chungnam.ac.kr
†Email address: rho@spht.saclay.cea.fr
‡Email address: a.wirzba@fz-juelich.de
§Email address: zahed@zahed.physics.sunysb.edu

tice QCD along the lines of the heavy-quark formalism is possible and will be discussed elsewhere [14].

The starting point in our analysis is the appropriate QCD action in Euclidean space with massless quarks

$$S=\int d^4x\left[\frac{1}{4}(F^a_{\mu\nu})^2+\overline{\psi}(\gamma_\mu\partial_\mu-\gamma_4\mu)\psi-iJ^a_\mu A^a_\mu\right], \quad (1)$$

and the colored current

$$J^a_\mu=g\overline{\psi}\gamma_\mu\frac{\lambda^a}{2}\psi. \quad (2)$$

In Euclidean space, our conventions are such that the γ-matrices are Hermitian with $\{\gamma_\mu,\gamma_\nu\}=2\delta_{\mu\nu}$. For sufficiently large μ, we will assume $g^2N_c\ll 1$. We have omitted gauge-fixing terms and ghost-fields. In what follows, we will analyze Eq. (1) in the one-loop approximation with the gluon field in the Feynman gauge. The approximation, as we shall show below, is equivalent to the resummation of the ladder graphs in the particle-particle or particle-hole graphs. The effects of screening will be dealt with by minimally modifying the gluon propagator, ignoring for simplicity vertex corrections as in [2]. The issue of gauge fixing dependence will be briefly discussed at the end.

In the one-loop approximation with screened gluons, the induced action is

$$S_\psi=\frac{g^2}{2}\int d^4x\,d^4y J^a_\mu(x)\mathcal{D}_{\mu\nu}(x-y)J^a_\nu(y)+\int d^4x\overline{\psi}\tilde{\partial}_\mu\gamma_\mu\psi, \quad (3)$$

where $\tilde{\partial}_\mu=(\partial_1,\partial_2,\partial_3,\partial_4-\mu)$. The screened gluon propagator $\{\mathcal{D}_{\mu\nu}\}=(\mathcal{D}_E,\mathcal{D}_M)$ will be approximated by

$$\mathcal{D}_{E,M}(x-y)=\int\frac{d^4q}{(2\pi)^4}\frac{1}{q^2+m^2_{E,M}}e^{-iq\cdot(x-y)}. \quad (4)$$

Perturbative arguments give $m_E^2/(g\mu)^2=m_D^2/(g\mu)^2\approx N_f/2\pi^2$ and $m_M^2/m_D^2\approx\pi|q_4|/|4\mathbf{q}|$, where m_D is the Debye mass, m_M is the magnetic screening generated by Landau damping and N_f the number of flavors [15].[1] Nonperturbative arguments suggest $m_E^2,m_M^2\to m_*^4/q^2$ [16] where for simplicity, the difference between electric and magnetic channels is ignored. We expect $\Lambda_{QCD}\ll m_*<m_E$ in the case $N_c=3$, as lattice simulations for the gluon propagator at finite μ are not yet available. We note that the perturbative screening vanishes at large N_c. In the Appendix, we show why the approximation (4), which simplifies the vector-structure of our analysis, yields exact results in the leading logarithm approximation.

To proceed further with Eq. (3) we need to Fierz rearrange the JJ term in Eq. (3). This is equivalent to summing ladder graphs with relevant quantum numbers. Specifically,

$$\begin{aligned}J^a_\mu(x)\mathcal{D}_{\mu\nu}(x-y)J^a_\nu(y)=g^2\sum_{\mathcal{O}}\mathcal{C}_{\mathcal{O}}[\overline{\psi}(x)\mathbf{M}_{\mathcal{O}}\psi(y)]\mathcal{D}(x-y)\\ \times[\overline{\psi}(y)\mathbf{M}_{\mathcal{O}}\psi(x)]\\ +g^2\sum_{\mathcal{O}'}\mathcal{C}_{\mathcal{O}'}[\overline{\psi}(x)\mathbf{M}_{\mathcal{O}'}\psi^c(y)]\\ \times\mathcal{D}(x-y)[\overline{\psi}^c(y)\mathbf{M}_{\mathcal{O}'}\psi(x)]\end{aligned} \quad (5)$$

with $\mathcal{C}_O=-1/9$ and $\mathcal{C}_C=+1/36$ for the operators

$$\begin{aligned}[\overline{\psi}(x)\mathbf{M}_O\psi(y)]&=\overline{\psi}_{\alpha,a,i}(x)\,\delta_{\alpha\beta}\delta_{ab}\delta_{ij}\psi_{\beta,b,j}(y),\\ [\overline{\psi}(x)\mathbf{M}_C\psi^c(y)]&=\overline{\psi}_{\alpha,a,i}(x)(\gamma_5)_{\alpha\beta}\varepsilon^I_{ab}\varepsilon^I_{ij}C\overline{\psi}^T_{\beta,b,j}(y),\end{aligned} \quad (6)$$

respectively, with $N_f=N_c=3$. These quantities involve matrices active in color $(a,b,\dots)$, flavor $(i,j,\dots)$ and Dirac space $(\alpha,\beta,\cdots)$. $\mathbf{M}_O$ is the vertex generator for particle-hole pairing in the 0^+ channel (i.e., Overhauser), while $\mathbf{M}_C$ is the vertex generator for particle-particle and hole-hole pairing in the color-flavor locked (CFL) channel (i.e., BCS). Only these two operators will be retained below, unless specified otherwise. The gluon-propagator in matter is

$$\mathcal{D}(x-y)=\frac{1}{2}\mathcal{D}_E(x-y)+\frac{1}{2}\mathcal{D}_M(x-y). \quad (7)$$

The weightings follow from minimal substitution in matter with 2 electric and 2 magnetic modes. We note that the present Fierz rearranging is particular, since it selects solely the $\mathbf{1}_c$ in the $\overline{qq}$ channel and the $\overline{\mathbf{3}}_c$ in the qq channel [17]. For arbitrary $N_c\geq 3$ and $N_f\geq 2$, the coefficients $-\frac{1}{9}$ and $\frac{1}{36}$ become, respectively, $-\frac{1}{2}(1-1/N_c)\cdot(1/N_f)$ and $(1/2N_c)\frac{1}{2}\cdot[1/\min(N_c,N_f)]$, where the single factors refer, in turn, to the results of the color Fierz rearranging, the flavor Fierz rearranging and, of course only for the second expression, the Fierz rearranging related to color-flavor locking.[2] To compare to the more conventional decompositions through $\mathbf{3}_c\times\overline{\mathbf{3}}_c=\mathbf{1}_c+\mathbf{8}_c$ for $\overline{qq}$ and $\mathbf{3}_c\times\mathbf{3}_c=\overline{\mathbf{3}}_c+\mathbf{6}_c$ for qq, with respective weights $-\frac{1}{2}[1-(1/N_c^2)]\cdot(1/N_f)$ and $[(N_c+1)/4N_c]\cdot\frac{1}{2}\cdot[1/\min(N_c,N_f)]$, we introduce also the vertex generator [2]

$$[\overline{\psi}(x)\mathbf{M}_B\psi^c(y)]=\overline{\psi}_{\alpha,a,i}(x)(\gamma_5)_{\alpha\beta}(\lambda_2)_{ab}(\tau_2)_{ij}C\overline{\psi}^T_{\beta,b,j}(y). \quad (8)$$

[1]Throughout we will refer to m_M abusively as the magnetic screening mass.

[2]At least partially, even if $N_f\neq N_c$, a locking can be achieved by Fierz rearranging the antisymmetric tensor in color times the corresponding one in flavor into the tensor $\mathbf{M}_{ai,bj}=\delta_{ai}\delta_{bj}-\delta_{aj}\delta_{bi}$ with the pertinent weight $1/\min(N_c,N_f)$ in the combined color-flavor space. The latter operator has $\frac{1}{2}n(n-1)$ eigenvalues $+1$, $\frac{1}{2}n(n+1)-1$ eigenvalues -1, one eigenvalue $n-1$, and $N_c\times N_f-n^2$ eigenvalues 0, where $n\equiv\min(N_c,N_f)$. Thus, in the BCS case, the fermion determinant (16) acquires the color-flavor weight $2n(n-1)$, while the corresponding value in the Overhauser case is the standard N_cN_f factor.

We note that Eq. (8) does not lock color and flavor as it stands; a color-flavor locking as described in footnote 2 still has to be performed, such that finally the corresponding coefficient becomes $\mathcal{C}_B=(N_c+1)/\{8N_c\min(N_f,N_c)\}$.[3] This brings about the important issue of whether Fierz rearranging is a unique operation on 4-Fermi interactions. The answer is no [22,23]. This nonuniqueness would of course not be important if an all-order calculation were to be performed for any Fierz rearranging set, but is of course relevant for truncated calculations as is the case in general. Each Fierzing corresponds to summing a specific class of ladder diagrams in the energy density, see e.g. [22,23].

Since the gap equations are inherently nonperturbative in content, it is hard to tell which Fierz rearranging to elect as a starting point in the many-body analysis. The conventional Fierz arranging decomposition corresponds to summing the nested gluon exchanges in the gap equation, while the unconventional decomposition does not have an immediate diagrammatic interpretation to our knowledge. Hence, the starting point of the conventional Fierz rearranging maybe improved upon by using systematically higher-order Feynman graphs and Ward identities. In contrast, the starting point of the unconventional Fierz rearranging maybe improved upon by using the random-phase-approximation. In weak-coupling, the gap equation is uniquely defined in the leading logarithm approximation. The result follows readily from the conventional Fierz rearranging decomposition to leading order.

Introducing a Hermitian bilocal field $\Sigma(x,y)$ and a non-Hermitian bilocal field $\Gamma(x,y)$, we may linearize the Fierz rearranged form of the JJ term by using the Hubbard-Stratonovich transformation, e.g.,

$$\exp\left(\frac{g^2}{18}\int d^4x\,d^4y[\bar{\psi}(x)\psi(y)]\mathcal{D}(x-y)[\bar{\psi}(y)\psi(x)]\right)$$
$$=\int d\Sigma(x,y)\exp\left(-S_\Sigma-\int d^4x\,d^4y\,\bar{\psi}(x)\Sigma(x,y)\psi(y)\right) \tag{9}$$

with

$$S_\Sigma=\frac{9}{2g^2}\int d^4x\,d^4y\frac{|\Sigma(x,y)|^2}{\mathcal{D}(x-y)} \tag{10}$$

and similarly for Γ. As a result, the action in the quark fields is linear and the functional integration can be performed. The result is the following effective action for the bilocal fields:

$$S=S_\Sigma+S_\Gamma-\tfrac{1}{2}\mathrm{Tr}\ln\mathbf{F}, \tag{11}$$

where

$$\mathbf{F}=\begin{pmatrix}\{\gamma\cdot\partial-\mu\gamma_4\}\delta(x-y)+\mathbf{M}_O\Sigma(x,y) & i\Gamma^\dagger(x,y)C^T\mathbf{M}_C\\ iC^T\Gamma(x,y)\mathbf{M}_C & \{\gamma\cdot\partial+\mu\gamma_4\}\delta(x-y)+\mathbf{M}_O\Sigma(x,y)\end{pmatrix}. \tag{12}$$

The factor of 1/2 in Eq. (11) is due to the occurrence of ψ and ψ^c through Fierz rearranging into $\mathbf{1}_c$ and $\mathbf{3}_c$ [17]. This renders naturally the Gorkov formalism applicable to the present problem even at $\mu=0$. Note that $\mathbf{M}_O=\mathbf{1}_C\times\mathbf{1}_F\times\mathbf{1}_D$ and $\mathbf{M}_C=\varepsilon_C^I\times\varepsilon_F^I\times\gamma_5$, with the subscripts C,F,D short for color, flavor and Dirac. We should stress that the effective action (11) is general. The third term is the Hartree contribution of the quarks to the ground state energy at large chemical potential, while the first two terms remove the double counting in the potential (i.e., Fock terms).

To analyze the Overhauser and BCS effects in parallel, we make simplifying *Ansätze* for the bilocal auxiliary fields. Since the unscreened gluon interaction in both cases peak in the forward direction, we may choose

$$\Sigma(x,y)=2\cos\left[P_\mu\left(\frac{x_\mu+y_\mu}{2}\right)\right]\sigma(x-y)=2\cos\left[P_\mu\left(\frac{x_\mu+y_\mu}{2}\right)\right]\int\frac{d^4q}{(2\pi)^4}e^{-iq\cdot(x-y)}F(q),$$

$$\Gamma(x,y)=2\cos\left[P_\mu\left(\frac{x_\mu-y_\mu}{2}\right)\right]g(x-y)=2\cos\left[P_\mu\left(\frac{x_\mu-y_\mu}{2}\right)\right]\int\frac{d^4q}{(2\pi)^4}e^{-iq\cdot(x-y)}G(q), \tag{13}$$

where $P_\mu=(\mathbf{P}_F,0)$ and $|\mathbf{P}_F|=2\mu$. $\mathbf{P}_F$ points in the original direction of one of the quarks. $F(q)$ and $G(q)$ are even functions, $F(q)$ is real, since $\Sigma(x,y)=\Sigma(y,x)^*$, and $G(q)$ is complex, since $\Gamma^\dagger(x,y)=\Gamma(y,x)^*$. The relative momentum q satisfies $|q|\leqslant|P/2|=\mu$. The bilocal field Γ characterizes a BCS pair of zero total momentum. Σ characterizes a wave of total momentum 2μ. This is the optimal choice for the momentum of the standing wave for which the holes contribute coherently

[3]In fact, expression (8) is the operator considered in Refs. [18,19] where color and flavor are uncoupled and only the two-flavor case is considered (see also [5,20]). Thus the corresponding coefficient is just $(N_c+1)/4N_c$, since the flavor-Fierzing factor can be ignored, as it eventually cancels against a corresponding factor resulting from the fermion determinant. Note, furthermore, that our color-flavor coupling scheme is different from the one recently introduced in Ref. [21] for arbitrary numbers of flavors.

to the wave formation. As a result the gap opens up at the Fermi surface, with μ as the divide between particles and holes. In both cases, the pairing involves a particle and/or hole at the opposite sides of the Fermi surface. Indeed, in terms of Eq. (13) the linear terms in the bilocal fields are

$$\int d^4x\, d^4y\, \overline{\psi}(x)\Sigma(x,y)\psi(y) = V_4 \int \frac{d^4q}{(2\pi)^4}\left[\overline{\psi}\left(-\frac{P}{2}+q\right)F(q)\psi\left(\frac{P}{2}+q\right)+\overline{\psi}\left(\frac{P}{2}+q\right)F(q)\psi\left(-\frac{P}{2}+q\right)\right] \tag{14}$$

(see Ref. [4]) and

$$\begin{aligned}
&\tfrac{1}{2}\int d^4x\, d^4y[\,\overline{\psi^c}(x) i\gamma_5 \Gamma(x,y)\psi(y) + \overline{\psi}(x)\Gamma^\dagger(x,y) i\gamma_5 \psi^c(y)] \\
&\quad = \tfrac{1}{2} V_4 \int \frac{d^4q}{(2\pi)^4}\left[\psi^T\left(-\frac{P}{2}-q\right) C i\gamma_5 G(q)\psi\left(\frac{P}{2}+q\right)+\overline{\psi}\left(\frac{P}{2}+q\right) iG^*(q)\gamma_5 C\overline{\psi}^T\left(-\frac{P}{2}-q\right)\right. \\
&\qquad \left.+\psi^T\left(\frac{P}{2}-q\right) C i\gamma_5 G(q)\psi\left(-\frac{P}{2}+q\right)+\overline{\psi}\left(-\frac{P}{2}+q\right) iG^*(q)\gamma_5 C\overline{\psi}^T\left(\frac{P}{2}-q\right)\right],
\end{aligned} \tag{15}$$

where V_4 is the 4-volume.

Following [4], we introduce fermion fields $\psi(\pm P/2+q)$ and $\psi^c(\pm P/2-q)$[4] that are independent integration variables in the relevant region of the momentum $|q| \ll |\mathbf{P}|/2$. Hence, the quark contribution around the Fermi surface can be integrated. The result is [25]

$$\det \mathbf{F} = \exp\left(V_4 \mathrm{Tr}\, \ln \begin{vmatrix} -i\tilde{Q}_{+,\mu}\sigma_\mu & F(q) & iG^*(q)\mathbf{M}_C & \mathbf{0} \\ F(q) & -i\tilde{Q}_{-,\mu}\overline{\sigma}_\mu & \mathbf{0} & -iG^*(q)\mathbf{M}_C \\ -iG(q)\mathbf{M}_C & \mathbf{0} & -i\tilde{Q}^*_{+,\mu}\overline{\sigma}_\mu & F(-q) \\ \mathbf{0} & iG(q)\mathbf{M}_C & F(-q) & -i\tilde{Q}^*_{-,\mu}\sigma_\mu \end{vmatrix} \right), \tag{16}$$

where $Q_\pm \equiv \pm P/2+q$ and $\tilde{Q}_\pm \equiv (\mathbf{Q}_\pm, Q_\pm^4 - i\mu)$. For each entry in momentum space q, the determinant in Eq. (16) is over an $(8\cdot N_c \cdot N_f)\times(8\cdot N_c\cdot N_f)$ matrix. The matrices $\sigma_\mu=(i\vec{\sigma},\mathbf{1})$ and $\overline{\sigma}_\mu=(-i\vec{\sigma},\mathbf{1})$ are defined in terms of the usual Pauli matrices $\vec{\sigma}$. The detailed analysis of the coupled problem (16) with the full fermion determinant will be discussed elsewhere [25].

III. GAP EQUATIONS

A qualitative understanding of the Overhauser effect versus the BCS effect can be achieved by studying the phases separately, and then comparing their energy densities at large quark density. Setting $G=0$ yields, for the Overhauser pairing, an energy density

$$\frac{S_\Sigma}{9V_4} = \frac{1}{g^2}\int d^4x \frac{|\sigma(x)|^2}{\mathcal{D}(x)} - 2\int \frac{d^4q}{(2\pi)^4}\ln\left[\frac{\tilde{Q}_+^2\tilde{Q}_-^2+2F^2\tilde{Q}_+\tilde{Q}_-+F^4}{\tilde{Q}_+^2\tilde{Q}_-^2}\right] \equiv \mathcal{S}_{\mathrm{pot},\Sigma}+\mathcal{S}_{\mathrm{kin},\Sigma}, \tag{17}$$

which is in agreement with the result derived originally in [4]. Setting $F=0$ yields, for the BCS pairing, an energy density

$$\frac{S_\Gamma}{36V_4} = \frac{1}{g^2}\int d^4x \frac{|g(x)|^2}{\mathcal{D}(x)} - \frac{2}{3}\int \frac{d^4q}{(2\pi)^4}\ln\left[\frac{\tilde{Q}_+^2\tilde{Q}_+^{*2}+2|G|^2\tilde{Q}_+\tilde{Q}_+^*+|G|^4}{\tilde{Q}_+^2\tilde{Q}_+^{*2}}\right] \equiv \mathcal{S}_{\mathrm{pot},\Gamma}+\mathcal{S}_{\mathrm{kin},\Gamma}, \tag{18}$$

which is similar to Eq. (17). In writing the last equation we have assumed that $|G(q\pm P)| \approx |G(\pm\mu)| \approx 0$. The gap equations for both cases follow by variation. The result is

$$F(p) = 2g^2\int \frac{d^4q}{(2\pi)^4}\mathcal{D}(p-q)\left(\frac{2F(q)(\tilde{Q}_+\tilde{Q}_-+F^2(q))}{\tilde{Q}_+^2\tilde{Q}_-^2+2F^2(q)\tilde{Q}_+\tilde{Q}_-+F^4(q)}\right) \tag{19}$$

---

[4]Note that we define $\psi^c(k)\equiv C\overline{\psi}^T(k)$ in terms of the Euclidean charge conjugation operator $C=\gamma_4\gamma_2$, whereas in Ref. [24] $\psi^c(k) \equiv C\overline{\psi}^T(-k)$. As usual, T stands for ''transposed.''

for the Overhauser gap, and

$$G(p)=\frac{2}{3}g^2\int\frac{d^4q}{(2\pi)^4}\mathcal{D}(p-q)\left(\frac{2G(q)(\tilde{Q}_+\tilde{Q}_+^*+|G(q)|^2)}{\tilde{Q}_+^2\tilde{Q}_+^{*2}+2|G(q)|^2\tilde{Q}_+\tilde{Q}_+^*+|G(q)|^4}\right) \tag{20}$$

for the BCS gap. If we were to use the antisymmetric vertex operator (8) then we would have $2g^2/3\to 4g^2/3$. For the latter, we have checked that the results (19) and (20) agree with the Bethe-Salpeter derivation in the ladder approximation to order μ^0. In our notations, the leading order effects are of order μ, the next to leading order effects are of order μ^0 and the next-to-next to leading order effects are of order μ^{-1}. For the screened gluon propagator we have the alternatives

$$\mathcal{D}(q)=\frac{1}{2}\frac{1}{q^2+m_E^2}+\frac{1}{2}\frac{1}{q^2+m_M^2},$$

$$\mathcal{D}(q)=\frac{1}{2}\frac{1}{q^2+im_*^2}+\frac{1}{2}\frac{1}{q^2-im_*^2}, \tag{21}$$

for the perturbative and nonperturbative assignments respectively.

The present construction is valid for an arbitrary number of colors with or without screening, thereby generalizing the original analysis in [4]. The outcome can be analyzed variationally, numerically or even analytically to leading logarithm accuracy. Using the following momentum decomposition around the fixed Fermi momentum P at the Fermi surface,

$$q_{||}=\frac{\mathbf{P}\cdot\mathbf{q}}{|\mathbf{P}|},\quad \mathbf{q}_\perp=\mathbf{q}-q_{||}\frac{\mathbf{P}}{|\mathbf{P}|}, \tag{22}$$

and assuming that the relevant values of the amplitudes of the bilocal fields are small (i.e., $F,|G|\ll\mu$), we may further simplify the kinetic part in the energy densities Eqs. (17),(18). Specifically,

$$\mathcal{S}_{\mathrm{kin},\Sigma}\approx -2\int\frac{d^4q}{(2\pi)^4}\ln\left[\frac{q_{||}^2+F^2(q)+\left\{q_4+\frac{q^2}{2i\mu}\right\}^2}{q_{||}^2+\left\{q_4+\frac{q^2}{2i\mu}\right\}^2}\right],$$

$$\mathcal{S}_{\mathrm{kin},\Gamma}\approx -\frac{2}{3}\int\frac{d^4q}{(2\pi)^4}\ln\left[\frac{q_4^2+|G(q)|^2+\left\{q_{||}+\frac{q^2}{2\mu}\right\}^2}{q_4^2+\left\{q_{||}+\frac{q^2}{2\mu}\right\}^2}\right]. \tag{23}$$

The simplified gap equations are

$$F(p)\approx 2g^2\int\frac{d^4q}{(2\pi)^4}\mathcal{D}(p-q)\left[\frac{F(q)}{q_{||}^2+F^2(q)+\left(q_4+\frac{q^2}{2i\mu}\right)^2}\right] \tag{24}$$

and

$$G(p)\approx\frac{2}{3}g^2\int\frac{d^4q}{(2\pi)^4}\mathcal{D}(p-q)\times\left[\frac{G(q)}{q_4^2+|G(q)|^2+\left(q_{||}+\frac{q^2}{2\mu}\right)^2}\right]. \tag{25}$$

For both pairings, the simplified energy densities $\overline{S}_{\Sigma,\Gamma}$ at their respective extrema are

$$\frac{\overline{S}_\Sigma}{9V_4}\approx 2\int\frac{d^4q}{(2\pi)^4}\left(\frac{1}{2}F\partial_F-1\right)\times\ln\left(1+\frac{F^2(q)}{q_{||}^2+\left(q_4+\frac{q^2}{2i\mu}\right)^2}\right),$$

$$\frac{\overline{S}_\Gamma}{36V_4}\approx\frac{2}{3}\int\frac{d^4q}{(2\pi)^4}\left(\frac{1}{2}|G|\partial_{|G|}-1\right)\times\ln\left(1+\frac{|G(q)|^2}{q_4^2+\left(q_{||}+\frac{q^2}{2\mu}\right)^2}\right).$$

We now proceed to evaluate F,G to leading logarithm accuracy.

IV. UNSCREENED CASE: LARGE N_c

In this section we consider the gap equations (24),(25) in the absence of screening. In the perturbative regime, we note that $m_{E,M}\sim 1/N_c$, and this approximation may be somehow justified in large N_c [4]. Hence,

$$F(p)\approx 2g^2\int\frac{d^4q}{(2\pi)^4}\frac{1}{(p-q)^2}\left[\frac{F(q)}{q_{||}^2+F^2(q)+\left(q_4+\frac{q^2}{2i\mu}\right)^2}\right] \tag{26}$$

and

$$G(p)\approx\frac{2}{3}g^2\int\frac{d^4q}{(2\pi)^4}\frac{1}{(p-q)^2}\times\left[\frac{G(q)}{q_4^2+|G(q)|^2+\left(q_{||}+\frac{q^2}{2\mu}\right)^2}\right]. \quad (27)$$

For the Overhauser pairing, if we assume the propagator to be static, the q_4 integration can be performed by a contour-integration with the constraint that

$$|q_\perp|^2\leqslant 2\mu\epsilon_q\equiv 2\mu\sqrt{q_{||}^2+F^2(q_{||})}. \quad (28)$$

Hence

$$F(p_{||})\approx h^2\int_0^\infty dq_{||}\frac{F(q_{||})}{\epsilon_q}\ln\left(1+\frac{2\mu\epsilon_q}{(p_{||}-q_{||})^2}\right) \quad (29)$$

with $h^2=g^2/4\pi^2$. In general, we have

$$h^2\equiv\frac{g^2N_c}{8\pi^2}\left(1-\frac{1}{N_c}\right),$$

$$h^2\equiv\frac{g^2N_c}{8\pi^2}\left(1-\frac{1}{N_c^2}\right), \quad (30)$$

for Fierz rearranging with $\mathbf{M}_C$ and $\mathbf{M}_B$ [4], respectively. Equation (29) is essentially a one-dimensional ''fish-diagram'' with logarithmically running couplings. This feature is preserved by screening as we will show below, in agreement with the recent renormalization group analysis in [5]. Following [20], the resulting equations are readily solved by defining the logarithmic scales $x\equiv\ln(2\mu/p_{||})$, $y\equiv\ln(2\mu/q_{||})$, $x_0\equiv\ln(2\mu/F_0)$, and rewriting

$$F(x)\approx h^2\left(2x\int_x^{x_0}dy\,F(y)-\int_x^{x_0}dy\,yF(y)+\int_0^x dy\,yF(y)\right). \quad (31)$$

Since $F''(x)=-2h^2F(x)$ with $F(x_0)=-F(0)$, then $F(x)=-F_0\cos(\sqrt{2}hx)$ [4,20]. The coefficient F_0 follows from $F'(x_0)=0$, with $\sqrt{2}hx_0=\pi$. Hence $F_0=F(x_0)$ and $x_0\equiv\ln(2\mu/F_0)=\pi/(\sqrt{2}h)$. Thus

$$F_0\sim 2\mu\exp\left\{-\frac{\pi}{\sqrt{2}h}\right\}, \quad (32)$$

which is exactly the result established in [4] using the $\mathbf{M}_C$ Fierz rearranging and elaborate variational arguments. Note that the pairing energy $F_0\ll\Lambda_\perp\ll\mu$ follows from an exponentially small region in transverse momentum (28) as required by momentum conservation, see Fig. 1(b). Typically $\Lambda_\perp=\sqrt{2\mu F_0}$ as originally suggested in [4].

For the BCS pairing, the transverse momentum is not restricted as shown in Fig. 1(a). This is best illustrated by noting that the BCS equation in Eq. (27) can be further simplified through the following substitution:

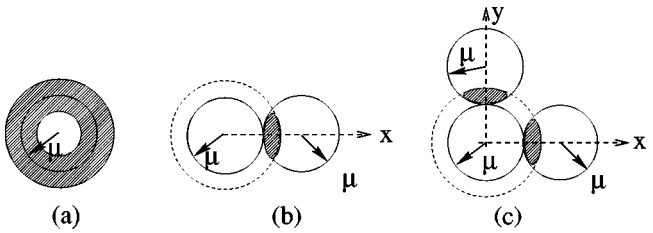

FIG. 1. (a) Fraction of the Fermi surface used in BCS pairing; (b) fraction of the Fermi surface used in the Overhauser pairing with one standing wave; (c) fractions of the Fermi surface used in the Overhauser pairing with two orthogonal standing waves.

$$q_{||}+\frac{\mathbf{q}^2}{2\mu}\rightarrow\left|\mathbf{q}+\frac{\mathbf{P}}{2}\right|-\mu. \quad (33)$$

This amounts to taking into account the effects of curvature around the fixed Fermi momentum $P/2$ defined by the standing wave. The trade (33) allows for a larger covering of the Fermi surface, although for $\Lambda_\perp=2\mu$ the terms that are dropped are only subleading for $q_{||}^2\ll q_\perp^2$. We have checked that this substitution does not not affect our analysis in the leading logarithm approximation. Shifting momenta to $Q=q+P/2$ and $K=p+P/2$ yields

$$G(K-P/2)\approx\frac{2}{3}g^2\int\frac{d^4Q}{(2\pi)^4}\mathcal{D}(K-Q)\times\left[\frac{G(Q-P/2)}{Q_4^2+|G(Q-P/2)|^2+(|\mathbf{Q}|-\mu)^2}\right]. \quad (34)$$

For a constant gap, the Q-integration diverges logarithmically. As most of the physics follows from $|\mathbf{Q}|=\mu$, this divergence can be regulated [18], with no effect on the leading-logarithm estimate of the pairing energy. Hence,

$$G(p_{||})\approx h_*^2\int_0^\infty dq_{||}\frac{G(q_{||})}{\epsilon_q}\ln\left(1+\frac{4\mu^2}{(p_{||}-q_{||})^2}\right), \quad (35)$$

with $\epsilon_q=\sqrt{q_{||}^2+|G(q_{||})|^2}$ following from the contour integration over Q_4. The prefactor reads $h_*^2=g^2/12\pi^2$, and in general[5]

$$h_*^2=\frac{g^2}{8\pi^2}\left(\frac{2}{N_c}\right)\frac{\min(N_f,N_c)-1}{2},$$

$$h_*^2=\frac{g^2}{8\pi^2}\left(1+\frac{1}{N_c}\right)\frac{\min(N_f,N_c)-1}{2}, \quad (36)$$

[5]In [20] and footnote 1 of [5] color and flavor are uncoupled. Hence $h_*^2=(g^2/8\pi^2)(1+1/N_c)$. In fact, this value can also be reproduced by the Fierz rearranging with $\mathbf{M}_B$ for the special case $N_f=3$.

corresponding to Fierz rearranging with $\mathbf{M}_C$ and $\mathbf{M}_B$ respectively. Notice the similarity between Eqs. (29) and (35), especially in the one-dimensional reduction of the equations. In terms of the logarithmic scales, the BCS equation reads [20]

$$G(x)\approx 2h_*^2\left(x\int_x^{x_0}dy\,G(y)+\int_0^x dy\,yG(y)\right). \tag{37}$$

Since $G''(x)=-2h_*^2G(x)$ with $G(0)=0$, then $G(x)=G_0\sin(\sqrt{2}h_*x)$. The coefficient G_0 follows from $G'(x_0)=0$ with $\sqrt{2}h_*x_0=\pi/2$. Hence $G_0=G(x_0)$ and, because of $x_0\equiv\ln(2\mu/G_0)$,

$$G_0\sim 2\mu\exp\left\{-\frac{\pi}{2\sqrt{2}h_*}\right\}. \tag{38}$$

Note that G_0 is enhanced relative to F_0, if $N_c=3$. They both become comparable for $N_c\geqslant 4$ in the $\mathbf{M_C}$-Fierz case with the Overhauser effect dominating at large N_c,[6] as originally suggested in [4].

We note that the i in Eq. (24) (Overhauser) versus no i in Eq. (25) (BCS) stems from the kinematical difference between the two pairings, hence a difference in the phase-space integration due to momentum conservation as shown in Figs. 1(a) and 1(b). In weak coupling, both gaps are exponentially small. The energy budget can be assessed by noting that the phase space volumes are of order: μ^2G_0 (BCS) and μF_0^2 (Overhauser). Hence, the energy densities are

$$\frac{S_\Sigma}{V_4}\approx-\mu F_0^3,\quad \frac{S_\Gamma}{V_4}\approx-\mu^2G_0^2. \tag{39}$$

In weak coupling, the BCS phase is energetically favored up to $N_c\sim 10$ in the unscreened case and for one standing wave for the $\mathbf{M}_C$ Fierz case. Under $\mathbf{M}_B$ Fierz rearranging, we have an additional constraint on the number of flavors, e.g., $N_f<\frac{2}{9}N_c$ for large N_c. Remember that further nestings of the Fermi surface by particle-hole pairing are still possible as shown in Fig. 1(c), causing a further reduction in S_Σ/V_4. A total nesting of the Fermi surface will bring about $4\pi\mu^2/\Lambda_\perp^2\approx\mu/F_0$ patches, hence $S_\Sigma/V_4\approx-\mu^2F_0^2$. The BCS phase becomes comparable to the Overhauser phase for $N_c\sim 4$ (see, however, footnote 6). Finally, we note that in strong coupling, both gaps are a fraction of μ.

V. SCREENED CASE: FINITE N_c

In the presence of electric and magnetic screening, which are important in matter, the situation changes significantly. While the original variational arguments in [4] were tailored for the unscreened case, our formulation which reproduces exactly their unscreened results in the leading logarithm approximation, generalizes naturally to the screened perturbative and nonperturbative cases in a minimal way. Indeed, using Eqs. (24),(25) and the pertinent transverse cutoffs, we obtain for perturbative screening,

$$\begin{aligned}F(p_{||})\approx&\frac{h^2}{6}\int_0^\infty dq_{||}\frac{F(q_{||})}{\sqrt{q_{||}^2+F^2(q_{||})}}\\&\times\ln\left\{\left(1+\frac{\Lambda_\perp^2}{(p_{||}-q_{||})^2+m_E^2}\right)^3\right.\\&\left.\times\left(1+\frac{\Lambda_\perp^3}{|p_{||}-q_{||}|^3+\frac{\pi}{4}m_D^2|p_{||}-q_{||}|}\right)^2\right\},\\G(p_{||})\approx&\frac{h_*^2}{6}\int_0^\infty dq_{||}\frac{G(q_{||})}{\sqrt{q_{||}^2+|G(q_{||})|^2}}\\&\times\ln\left\{\left(1+\frac{\Lambda_\perp^2}{(p_{||}-q_{||})^2+m_E^2}\right)^3\right.\\&\left.\times\left(1+\frac{\Lambda_\perp^3}{|p_{||}-q_{||}|^3+\frac{\pi}{4}m_D^2|p_{||}-q_{||}|}\right)^2\right\},\end{aligned} \tag{40}$$

and for nonperturbative screening

$$\begin{aligned}F(p_{||})\approx&h^2\int_0^\infty dq_{||}\frac{F(q_{||})}{\sqrt{q_{||}^2+F^2(q_{||})}}\ln\left|1+\frac{\Lambda_\perp^2}{(p_{||}-q_{||})^2+im_*^2}\right|,\\G(p_{||})\approx&h_*^2\int_0^\infty dq_{||}\frac{G(q_{||})}{\sqrt{q_{||}^2+|G(q_{||})|^2}}\\&\times\ln\left|1+\frac{\Lambda_\perp^2}{(p_{||}-q_{||})^2+im_*^2}\right|,\end{aligned} \tag{41}$$

where the transverse cutoffs are $\Lambda_\perp=\sqrt{2\mu\epsilon_q}$ (Overhauser) and $\Lambda_\perp=2\mu$ (BCS) respectively. The cutoffs are exactly fixed in weak coupling, and reflect on the fractions of the Fermi surface used in the pairing.

In the BCS case, the transverse cutoff is large. Hence $\Lambda_\perp>m_E,m_M$ and the logarithm in Eq. (40) may not be expanded. Dropping 1, we obtain to leading logarithm accuracy,

$$G_0\approx\left(\frac{4\Lambda_\perp^6}{\pi m_E^5}\right)e^{-\sqrt{3}\pi/2h_*}. \tag{42}$$

[6]In the $\mathbf{M}_B$-Fierz case, the Overhauser effect only dominates in the large N_c limit, if $N_f<\frac{1}{2}N_c$.

The result for the BCS gap is the same as the one reached in [20,19,18],[7] if we were to Fierz rearrange with $\mathbf{M}_B$ instead of $\mathbf{M}_C$. Note that Eq. (42) is smaller than Eq. (38) as expected. For nonperturbative screening, the result is

$$G_0 \approx \Lambda_\perp e^{-(2/h_*^2)\{\ln(1+\Lambda_\perp^4/m_*^4)\}^{-1}}, \tag{43}$$

with $\Lambda_\perp/m_* = 2\mu/m_* \gg 1$.

In the Overhauser case, the transverse cutoff is reduced in comparison to the BCS case due to momentum conservation for fixed 3-momentum for the standing wave. The equation can be rearranged into the form

$$F(p_{||}) \approx \frac{h^2}{6}\int_0^\infty dq_{||}\frac{F(q_{||})}{\epsilon_q}\ln\left(\frac{2\mu\epsilon_q}{(p_{||}-q_{||})^2}\right) + \frac{5h^2}{6}\int_0^\infty dq_{||}\frac{F(q_{||})}{\epsilon_q}\ln\left(\frac{2\mu\epsilon_q}{(p_{||}-q_{||})^2+m_E^2}\right), \tag{44}$$

where we have approximated $\pi m_D^2/4 \sim m_E^2$ and used static, but perturbatively screened propagators. The effects of Landau damping through the magnetic gluons result into an unscreened interaction but with a reduced strength $h^2 \to h^2/6$. Equation (44) can be solved to leading logarithm accuracy using the logarithmic scales as defined above. Specifically, for $x < x_m \equiv \ln(2\mu/m_E)$, we get

$$F(x) \approx h^2\left(2x\int_x^{x_L} dy\, F(y) - \int_x^{x_L} dy\, yF(y) + \int_0^x dy\, yF(y)\right) \tag{45}$$

as in the unscreened case with $x_L = x_0$, and for $x > x_m$

$$F(x) \approx \frac{h^2}{6}\left(2x\int_x^{x_R} dy\, F(y) - \int_x^{x_R} dy\, yF(y) + \int_0^x dy\, yF(y)\right) + \mathcal{C}. \tag{46}$$

Here $x_{L,R} \equiv \ln(2\mu/F_{L,R})$ and the constant $\mathcal{C}$ is given by

$$\mathcal{C} = \frac{5h^2}{6}\int_0^\infty dq_{||}\frac{F(q_{||})}{\epsilon_q}\ln\left(\frac{2\mu\epsilon_q}{\max(q_{||}^2, m_E^2)}\right). \tag{47}$$

The solution to Eqs. (45),(46) is

$$F(x) = F_L\cos(\sqrt{2}h(x-x_L)) \quad \text{for } x < x_m,$$
$$F(x) = F_R\cos(h(x-x_R)/\sqrt{3}) \quad \text{for } x > x_m. \tag{48}$$

We note that for $x < x_m$ or $p_{||} > m_E$, screening can be ignored to leading logarithm accuracy and $x_L = \pi/\sqrt{2}h$ as before. For $x > x_m$ or $p_{||} < m_E$, screening cannot be ignored to leading logarithm accuracy. Continuity at x_m fixes x_R, so that

$$F_R = F_L\frac{\cos\{\sqrt{2}h(x_m - x_L)\}}{\cos\{h(x_m - x_R)/\sqrt{3}\}} = e^{-\pi/\sqrt{2}h}\frac{\cos\left\{\sqrt{2}h\ln\left(\frac{2\mu}{m_E}\right) - \pi\right\}}{\cos\left\{h\left[\ln\left(\frac{2\mu}{m_E}\right) - \ln\left(\frac{2\mu}{F_R}\right)\right]\Big/\sqrt{3}\right\}}. \tag{49}$$

Equation (49) defines a transcendental equation for $F_R/2\mu$ as a function of N_f, N_c and h (equivalently μ), i.e.,

$$\frac{F_R}{2\mu} \approx -e^{-\pi/\sqrt{2}h}\frac{\cos\left\{\frac{h}{\sqrt{2}}\ln\left(\frac{N_c}{N_f h^2}\right)\right\}}{\cos\left\{\frac{h}{\sqrt{3}}\ln\left(\sqrt{\frac{N_c}{N_f h^2}}\frac{F_R}{2\mu}\right)\right\}}, \tag{50}$$

where we have used $m_E/2\mu \approx h\sqrt{N_f/N_c}$, with

$$\frac{1}{h^2} \approx \frac{8\pi^2}{N_c g^2} \approx \frac{11}{3}\ln\left(\frac{\mu}{\Lambda_{QCD}}\right) + \frac{17}{11}\ln\ln\left(\frac{\mu}{\Lambda_{QCD}}\right) \tag{51}$$

to two loops. For fixed N_c and in weak coupling ($h \to 0$), there is no solution to Eq. (50) as can be seen by inspection. This corresponds to a screening mass with power suppression, e.g. $m_E/\mu \approx h$. However, a solution can be found in weak coupling but large N_c, when approximately

$$e^{-\pi/\sqrt{2}h}\sqrt{\frac{N_c}{N_f h^2}} \approx 1 \tag{52}$$

for which $F_R \approx F_L$. Through N_c, this corresponds to a screening mass with exponential suppression, e.g., $m_E/\mu \approx e^{-\pi/\sqrt{2}h}$.

To assess the minimal value of N_c for which there is a solution to Eq. (50), it is useful to note that the solution (48) is invariant under the shift

$$x \to x + \ln\left(\frac{\Lambda_\perp}{2\mu}\right) \tag{53}$$

with similar shifts in the scales $x_{m,L,R}$, implying the existence of a family of solutions that depend parametrically on $x_{m,L,R}$ and $\Lambda_\perp$. The harmonic equation satisfied by $F(x)$ is scale invariant, hence of the renormalization group type.[8]

[7] Modulo the dimensionless constant b_0' in [18].

[8] Indeed, $f(x) = -F'(x)/F(x)$ satisfies $f'(x) = f^2(x) + 2h^2$ for $x < x_m$ and $f'(x) = f^2(x) + h^2/3$ for $x > x_m$, which are the renormalization group equations derived in [5], after the identification $h \to h/\sqrt{2}$. A similar observation extends to the BCS case, where $g(x) = -G'(x)/G(x)$ satisfies $g'(x) = g^2(x) + 2h_*^2$ (unscreened) and $g'(x) = g^2(x) + h_*^2/3$ (screened), in agreement with the renormalization group equations derived in [20].

The scale x_R is fixed in terms of $x_{L,m}$ by demanding that the logarithmic derivatives of Eq. (48) (with pertinent shifts) match at x_m. Thus

$$\frac{1}{\sqrt{6}}\tan\left(\frac{h}{\sqrt{3}}(x_m-x_R)\right)=\tan(\sqrt{2}h(x_m-x_L)), \tag{54}$$

with

$$x_R=-\frac{\sqrt{3}}{h}\{\arctan[\sqrt{6}\tan(\sqrt{2}h(x_m-x_L))]+\mathrm{mod}\,\pi\}+x_m. \tag{55}$$

The lower bound on N_c or equivalently the upper bound on the electric mass follows from

$$m_E\equiv\Lambda_\perp e^{-x_m}=\left(\frac{\Lambda_\perp^2}{2\mu}\right)\left(\frac{2\mu}{\Lambda_\perp}\right)e^{-x_m}\leqslant 2\mu\left(\frac{\Lambda_{||}}{\Lambda_\perp}\right)e^{-x_m}$$
$$\equiv 2\mu e^{-x_{||}-x_m}, \tag{56}$$

where $\Lambda_\perp$ and $\Lambda_{||}$ are now exponentially small scales characterizing the spread in $p_\perp$ and $p_{||}$. The inequality in Eq. (56) follows from the geometrical constraint $\Lambda_{||}\geqslant\Lambda_\perp^2/2\mu$ discussed above [see Eq. (28) and also Fig. 1(b)]). Up to the rescaling (53), the maximum $\Lambda_{||}$ for which there is a solution (48) with positive semi-definite gap, corresponds to $F(x_{||})=0$, i.e., $x_{||}=x_R+\sqrt{3}\pi/2h$. (The alternative solution $x_{||}=x_L+\sqrt{2}\pi/4h$ does not generate a maximum bound.) After inserting the latter and Eq. (55) into $\hat{c}\equiv\sqrt{2}h\,\min(x_{||}+x_m)$, we determine the minimum as $\hat{c}\approx 2.5051$ and the lower bound for N_c (upper bound for the electric mass m_E) as

$$\frac{N_c}{N_f}\geqslant h^2 e^{\sqrt{2}\hat{c}/h}. \tag{57}$$

This result is in overall agreement with a recent renormalization group estimate [5].[9] In particular, for $\mu=3\Lambda_{QCD}$, we find $N_c\geqslant 334N_f$.

The case of nonperturbative screening can be addressed similarly by noting that Eq. (44) is now

$$F(p_{||})\approx\frac{h^2}{2}\int_0^\infty dq_{||}\frac{F(q_{||})}{\epsilon_q}\ln\left(\frac{(2\mu\epsilon_q)^2}{(p_{||}-q_{||})^4+m_*^4}\right). \tag{58}$$

For $x<x_m$ or $p_{||}>m_*$ the screening in Eq. (58) is inactive. Hence $F(x)=-F_L\cos(\sqrt{2}hx)$, while for $x>x_m$ or $p_{||}<m_*$ the screening overwhelms the leading logarithm accuracy with $F(x)=\mathrm{const}$. Continuity at x_m requires that $x_m=x_L$. Hence

$$m_*=2\mu e^{-\pi/\sqrt{2}h}, \tag{59}$$

which is the maximum tolerated nonperturbative screening mass for an Overhauser pairing to take place.

[9]After the identification $h\to h/\sqrt{2}$ and $\mu\to 2\mu$ in the prefactor of m_E in [5].

Finally, we can qualitatively analyze the effects of temperature on the Overhauser effect by considering the distribution of quasiparticles at the Fermi surface. At finite temperature T, the pairing energy becomes

$$F(p_{||})\approx\frac{h^2}{6}\int_0^\infty dq_{||}\frac{F(q_{||})}{\epsilon_q}\ln\left(\frac{2\mu\epsilon_q}{(p_{||}-q_{||})^2}\right)$$
$$\times\tanh\left(\frac{\epsilon_q}{2T}\right)+\frac{5h^2}{6}\int_0^\infty dq_{||}\frac{F(q_{||})}{\epsilon_q}$$
$$\times\ln\left(\frac{2\mu\epsilon_q}{(p_{||}-q_{||})^2+m_E(T)^2}\right)\tanh\left(\frac{\epsilon_q}{2T}\right), \tag{60}$$

with the temperature dependent screening mass [15]

$$m_E^2(T)=m_E^2+\left(N_c+\frac{N_f}{2}\right)\frac{g^2T^2}{3}. \tag{61}$$

Even at large N_c the screening mass is finite. We conclude that at finite temperature, the Overhauser pairing is rapidly depleted by screening for any value of N_c.

VI. PAIRING IN LOWER DIMENSIONS

The results we have derived depend on the number of dimensions. Indeed, the QCD analysis we have carried out when applied to 1+1 dimensions yield the following energy gaps:

$$F(p)\approx h^2\int_0^\infty dq\frac{F(q)}{\epsilon_q}\frac{1}{(p-q)^2+m_E^2},$$

$$G(p)\approx h_*^2\int_0^\infty dq\frac{G(p)}{\epsilon_q}\frac{1}{(p-q)^2+m_E^2}, \tag{62}$$

with the replacement $g^2/8\pi^2\to g^2/2\pi$ in h^2 and h_*^2. Remember that $F(q)$ and $G(q)$ have been defined as even functions. In deriving Eq. (62) we have followed the same logic as in 3+1 dimensions, thereby ignoring self-energy insertion on the quark line, and the gauge-fixing dependence on the gluon propagator. While these two effects cancel in color singlet states (Overhauser) [26], they usually do not in color-non-singlet states (BCS) except for the case of $N_c=2$ [22]. In 1+1 dimensions $g^2/2\pi$ has mass dimension, and there is only electric screening with $m_E^2\approx N_f g^2\ln(\mu/g)$. Clearly,

$$F_0\approx\Lambda e^{-m_E^2/h^2}\gg G_0\approx\Lambda e^{-m_E^2/h_*^2}. \tag{63}$$

The dominance of the Overhauser effect over the BCS effect whatever N_c, stems from the fact that the Fermi surface reduces to 2 points ($\pm\mu$) in 1+1 dimensions, with no phase space reduction for the former. Since both the Overhauser and BCS phase break spontaneously chiral symmetry at finite density, the existence of the Overhauser phase may rely ultimatly on large N_c. The Overhauser effect is dominant in the Schwinger model where $G_0=0$ because of the repulsive

character of the Coulomb interaction,[10] confirming the results in [7–9]. The case of QCD in $2+1$ dimensions will be discussed elsewhere.

VII. CONCLUSIONS

We have constructed a Wilsonian effective action for various scalar-isoscalar excitations around the Fermi surface. Our analysis in the decoupled mode shows that in weak coupling the Overhauser effect can overtake the BCS effect only at large N_c in the scalar-isoscalar channel, in agreement with a recent renormalization group result [5]. The BCS pairing is more robust to screening than the Overhauser pairing in weak coupling. The BCS analysis was carried out for both the CFL and the antisymmetric arrangements for arbitrary $N_c \geqslant 3$, $N_f \geqslant 2$, ignoring the superconducting penetration lengths since the electric and magnetic screening lengths are smaller than the London and Pippard lengths (for type-I superconductors). In strong coupling, the Overhauser effect appears to be comparable to the BCS effect, especially if multiple standing waves are used, allowing for further cooperative pairing between adjacent patches. This is particularly relevant for pairings with large energy gaps which are expected to take place at a few times nuclear matter density [19].

Our effective action is better suited to the use of variational approximations as discussed in [4], and leads naturally to exact integral equations by variations, especially in the presence of interactions with retardation and screening. It would be interesting to repeat our analysis at nonasymptotic densities using instanton-generated vertices to address the Overhauser effect. Indeed, for instantons the cutoff is fixed from the onset by their inverse size. As we have shown here, the Overhauser pairing, much like the BCS pairing by magnetic forces [20], relies on scattering between pairs in the forward direction that is kinematically suppressed in the transverse directions (in fact exponentially suppressed [4]). Since the instanton interaction is nearly uniform over the Fermi sphere, we expect a geometrical enhancement in the BCS pairing in comparison to the Overhauser pairing. We recall that in the latter the interaction is enhanced by a factor of order N_c. Which one dominates at a few times nuclear matter density and $N_c=3$ is not clear *a priori*. Instantons in the vacuum crystallize for $N_c \geqslant 20$ [27] in the quenched approximation, and $3<N_c<20$ in the unquenched case. The crystallization is likely to be favored by finite μ as the quarks are forced to line up along the forward x_4 direction.

It is amusing to note that the crystal phase breaks color, flavor, and translational symmetry spontaneously, with the occurrence of color and flavor density waves. In many ways, this situation resembles the one encountered with dense Skyrmions [10] (strong coupling), suggesting the possibility of a smooth transition. In the process, color and flavor, respectively, may get misaligned [28], resulting into color-flavor-locked charge density waves in a normal (large gaps) phase. The Skyrmion crystal at low density may smoothly transmute to a qualiton crystal at intermediate densities, with crystalline structure commensurate with the number of patches on the Fermi surface. We note that the crystalline structure in $3+1$ dimensions may only show up as rapid variations in the response functions at momentum 2μ. This is not the case in $1+1$ and $2+1$ dimensions [3].

Although we have carried out the analysis using Feynman gauge with minimal changes for the electric and magnetic screening, we expect our estimates of the gap energies to be reliable since a close inspection of the equations we derived when reinterpreted in Minkowski space, shows that the quoted results originate from the forward scattering amplitude of quarks around the Fermi surface. The latter is infrared sensitive in the unscreened case and gauge independent, the exception being in $1+1$ dimension [26,22]. The similarity between forward particle-particle and particle-hole scattering resembles the similarity between forward Compton and Bhabha scattering. This is what makes 2μ and opposite sides to the Fermi surface so special between a particle and a hole.

Finally, it is amusing to note that following either the Overhauser or BCS pairing, the quark eigenvalues of the QCD Dirac operator would suggest a novel rearrangement that is characterized by novel spectral sum rules. They will be reported elsewhere. Our use of the effective action at the Fermi surface is more than a convenience for the study of QCD at large quark chemical potential. Indeed, given the shortcomings faced by important samplings in lattice Monte Carlo simulations at finite quark chemical potential, and also given the importance of Pauli blocking for the non-surface modes, we believe that a convenient formulation of QCD on the lattice should make use of fermionic fields projected onto the Fermi surface, much like the ones used in the present work, and in the spirit of the heavy-quark formalism [14].

ACKNOWLEDGMENTS

A.W. and I.Z. would like to thank Gerry Brown and Edward Shuryak for discussions. I.Z. is grateful to Larry McLerran, Robert Pisarski, Dam Son, and Frank Wilczek for useful discussions. We have benefitted from conversations with Deog Ki Hong, Steve Hsu, and Maciek Nowak, and from assistance from Chang Hwan Lee. B.Y.P., M.R. and I.Z. acknowledge the hospitality of KIAS where part of this work was done, and A.W. the hospitality of the NTG group at Stony Brook. This work was supported in part by KOSEF 985-0200-001-2, US-DOE DE-FG-88ER40388 and DE-FG02-86ER40251.

APPENDIX

The comparison of the exact and simplified in-medium gluon propagator

According to Eq. (6.51) of [15] and Eq. (10) of [19], the in-medium (Minkowski-space) gluon-propagator in a general covariant gauge reads (modulo an overall phase factor)

$$\mathcal{D}_{\mu\nu}(q)=i\frac{P^T_{\mu\nu}}{q^2-G}+i\frac{P^L_{\mu\nu}}{q^2-F}-i\xi\frac{P^{GF}_{\mu\nu}}{q^2}, \qquad \text{(A1)}$$

[10] In the Schwinger model $m_E^2=g^2/2\pi$ independently of μ.

where $F \equiv m_D^2 = m_E^2 = (N_f/2\pi^2) g^2 \mu^2$ and $G \equiv m_M^2 = (\pi/4)(q_0/|\mathbf{q}|) m_D^2$. The propagator contains the gauge parameter ξ, which must not appear in physical results. The projectors appearing in Eq. (A1) read

$$P^T_{\mu\nu} = (1-g_{\mu 0})(1-g_{\nu 0})\left(-g_{\mu\nu} - \frac{q_\mu q_\nu}{\mathbf{q}^2}\right), \tag{A2}$$

$$P^L_{\mu\nu} = -g_{\mu\nu} + \frac{q_\mu q_\nu}{q^2} - P^T_{\mu\nu}, \tag{A3}$$

$$P^{GF}_{\mu\nu} = \frac{q_\mu q_\nu}{q^2}, \tag{A4}$$

where $q^2 = q^{02} - \mathbf{q}^2$ and $g_{\mu\nu} = g^{\mu\nu} = \mathrm{diag}(1,-1,-1,-1)$ for $\mu,\nu = 0,1,2,3$. The transverse projector can be written as

$$P^T_{\mu 0} = P^T_{0\nu} = 0, \tag{A5}$$

$$P^T_{ij} = P^T_{ji} = \delta_{ij} - \hat{\mathbf{q}}_i \hat{\mathbf{q}}_j, \tag{A6}$$

where $\hat{\mathbf{q}}_i \equiv q_i/|\mathbf{q}|$. Equation (A1) should be compared with the simplified form

$$\mathcal{D}_{\mu\nu}(q) = i\frac{1}{2}\frac{-g_{\mu\nu}}{q^2 - G} + i\frac{1}{2}\frac{-g_{\mu\nu}}{q^2 - F}, \tag{A7}$$

which is the analog in Minkowski space of the screened perturbative gluon propagator in Euclidean space used here in Eqs. (3), (7) and (21). We now proceed to show that Eqs. (A1) and (A7) yield equivalent results in the leading logarithm approximation, although the analysis is simpler using Eq. (A7).

The three-momentum can be split into the Fermi-momentum $\mathbf{P}$ and a momentum $\vec{l}$ measured relative to the Fermi surface,

$$|\mathbf{q}| = \left|\frac{\mathbf{P}}{2} + \vec{l}\right| = \mu + l_{||} + \frac{l_\perp^2}{2\mu} + \mathcal{O}(1/\mu^2), \tag{A8}$$

where $l_{||}$ and $l_\perp$ are the projections of the relative momentum in the direction of and orthogonal to the Fermi-momentum $\mathbf{P}$, respectively. Because of the decomposition (A8), we have, modulo $1/\mu^2$ corrections, $q^2 = q_0^2 - \mathbf{q}^2 \approx -\mathbf{q}^2$ and we can simplify the longitudinal projector as follows (see [19]):

$$P^L_{\mu\nu} \approx -g_{\mu 0} g_{\nu 0}. \tag{A9}$$

Finally we will use that

$$\delta^{ij} P^T_{ij} = 2, \tag{A10}$$

$$\hat{\mathbf{q}}\cdot\hat{\mathbf{Q}}\hat{\mathbf{k}}\cdot\hat{\mathbf{Q}} = -\tfrac{1}{2}(1 - \hat{\mathbf{q}}\cdot\hat{\mathbf{k}}) + \mathcal{O}(1/\mu), \tag{A11}$$

where $Q \equiv k - q$. The second formula can be derived with the help of Eq. (A8) applied to $|\mathbf{k}|$, $|\mathbf{q}|$ and $|\mathbf{Q}| = |\mathbf{k} - \mathbf{q}|$, i.e., $|\mathbf{Q}|^2 = |\mathbf{k} - \mathbf{q}|^2 \approx 2\mu^2(1 - \hat{\mathbf{q}}\cdot\hat{\mathbf{k}})$ and $\hat{\mathbf{q}}\cdot\mathbf{Q}\hat{\mathbf{k}}\cdot\mathbf{Q} = (|\mathbf{k}|\hat{\mathbf{q}}\cdot\hat{\mathbf{k}} - |\mathbf{q}|)(|\mathbf{k}| - |\mathbf{q}|\hat{\mathbf{q}}\cdot\hat{\mathbf{k}}) \approx -\mu^2(1 - \hat{\mathbf{q}}\cdot\hat{\mathbf{k}})^2$.

The Dirac structure of the gap equation (9) of [19] reads

$$\begin{aligned} A^{\mu\nu} &\equiv \tfrac{1}{2}\mathrm{Tr}[\,\gamma^\mu \tfrac{1}{2}(1 - s_R \gamma^0\gamma^m \hat{\mathbf{q}}^m)\,\gamma^\nu \tfrac{1}{2}(1 + s_L \gamma^0\gamma^n \hat{\mathbf{k}}^n)\,] \\ &= \tfrac{1}{2} g^{\mu\nu} + \frac{s_L}{2}(g^{\mu n} g^{\nu 0} - g^{\mu 0} g^{\nu n})\hat{\mathbf{k}}^n \\ &\quad + \frac{s_R}{2}(g^{\mu m} g^{\nu 0} - g^{\mu 0} g^{\nu m})\hat{\mathbf{q}}^m + \frac{s_R s_L}{2}(2 g^{\mu 0} g^{\nu 0}\delta^{mn} \\ &\quad - g^{\mu\nu}\delta^{mn} - g^{\mu m} g^{\nu n} - g^{\mu n} g^{\nu m})\hat{\mathbf{q}}^m \hat{\mathbf{k}}^n, \end{aligned} \tag{A12}$$

where $s_L = s_R = \pm 1$ for the gap and $s_L = -s_R = \pm 1$ for the antigap. The prefactor $\frac{1}{2}$ in Eq. (A12) can be traced back to the division by the Dirac trace on the left-hand side of the gap equation, namely to the division by $\mathrm{Tr}[\,\frac{1}{2}(1 + s_L \gamma^0\gamma^n \hat{\mathbf{k}}^n)\,] = 2$; see Eq. (9) of [19].

Using the projectors of $\mathcal{D}_{\mu\nu}(k-q)$ as given in Eq. (A1), we get

$$A^{\mu\nu} P^L_{\mu\nu} = -A^{00} = -\tfrac{1}{2}(1 + s_R s_L \hat{\mathbf{q}}\cdot\mathbf{k}) \tag{A13}$$

for the longitudinal (electric) case. Assuming as in [19] that $\hat{\mathbf{q}}\cdot\hat{\mathbf{k}} \equiv \cos(\theta) \approx 1$ in the *numerators* of the gap equation, we get the weight -1 for the longitudinal contribution to the gap and 0 for the longitudinal contribution to the antigap. In summary,

$$A^{\mu\nu} P^L_{\mu\nu} \approx \begin{cases} -1 & \text{(gap)}, \\ 0 & \text{(antigap)}. \end{cases} \tag{A14}$$

Furthermore, we have using Eq. (A11)

$$\begin{aligned} A^{\mu\nu} P^T_{\mu\nu} &= \tfrac{1}{2} g^{ij} P^T_{ij} + \frac{s_R s_L}{2}(-2P^T_{mn} + \delta^{ij} P^T_{ij}\delta^{mn})\hat{\mathbf{k}}^n \hat{\mathbf{q}}^m \\ &= -1 + s_R s_L(\hat{\mathbf{k}}\cdot\hat{\mathbf{q}} - \hat{\mathbf{k}}\cdot\hat{\mathbf{q}} + \hat{\mathbf{k}}\cdot\hat{\mathbf{Q}}\hat{\mathbf{q}}\cdot\hat{\mathbf{Q}}) \\ &\approx -1 - \tfrac{1}{2} s_R s_L + \tfrac{1}{2} s_R s_L \hat{\mathbf{k}}\cdot\hat{\mathbf{q}} \end{aligned} \tag{A15}$$

for the transverse (magnetic) case. Under the approximation $\hat{\mathbf{k}}\cdot\hat{\mathbf{q}} \approx 1$, we get for the gap case $-\frac{3}{2} + \frac{1}{2}\hat{\mathbf{k}}\cdot\hat{\mathbf{q}} \approx -1$ and for the antigap case $-\frac{1}{2} - \frac{1}{2}\hat{\mathbf{k}}\cdot\hat{\mathbf{q}} \approx -1$, i.e.,

$$A^{\mu\nu} P^T_{\mu\nu} \approx -1. \tag{A16}$$

Finally,

$$A^{\mu\nu}P^{GF}_{\mu\nu}=\tfrac{1}{2}\frac{g^{\mu\nu}Q_\mu Q_\nu}{Q^2}+\frac{s_R s_L}{2}\left(2\frac{Q^0Q^0}{Q^2}\hat{\mathbf{k}}\cdot\hat{\mathbf{q}}-2\frac{\mathbf{Q}\cdot\hat{\mathbf{k}}\mathbf{Q}\cdot\hat{\mathbf{q}}}{Q^2}-\frac{Q^2}{Q^2}\hat{\mathbf{k}}\cdot\hat{\mathbf{q}}\right)$$

$$=\tfrac{1}{2}-\frac{s_R s_L}{2}\hat{\mathbf{k}}\cdot\hat{\mathbf{q}}+s_R s_L\left(\hat{\mathbf{k}}\cdot\hat{\mathbf{q}}\frac{Q^{02}}{Q^2}-\frac{\mathbf{Q}\cdot\hat{\mathbf{k}}\mathbf{Q}\cdot\hat{\mathbf{q}}}{Q^2}\right)$$

$$\approx\tfrac{1}{2}-\frac{s_R s_L}{2}\hat{\mathbf{k}}\cdot\hat{\mathbf{q}}+s_R s_L\left(-\frac{\mathbf{Q}\cdot\hat{\mathbf{k}}\mathbf{Q}\cdot\hat{\mathbf{q}}}{-\mathbf{Q}^2}\right)$$

$$\approx\tfrac{1}{2}-\frac{s_R s_L}{2}\hat{\mathbf{k}}\cdot\hat{\mathbf{q}}+s_R s_L(\tfrac{1}{2}\hat{\mathbf{k}}\cdot\hat{\mathbf{q}}-\tfrac{1}{2})$$

$$=\tfrac{1}{2}(1-s_R s_L), \tag{A17}$$

where $Q^2\approx-\mathbf{Q}^2$ and Eq. (A11) was used. Note that the gauge-fixing dependence vanishes for the gap and gives a weight factor $+1$ for the antigap:

$$A^{\mu\nu}P^{GF}_{\mu\nu}\approx\begin{cases}0 & \text{(gap)},\\ +1 & \text{(antigap)}.\end{cases} \tag{A18}$$

If $A^{\mu\nu}$ is contracted with $-\frac{1}{2}g_{\mu\nu}$, valid for both the magnetic and electric term of the simplified form of the gluon-propagator (A7), we get

$$A^{\mu\nu}\frac{-1}{2}g_{\mu\nu}=-1+\frac{s_R s_L}{2}(-g^{00}\hat{\mathbf{q}}\cdot\hat{\mathbf{k}}+2\hat{\mathbf{q}}\cdot\hat{\mathbf{k}}+\tfrac{1}{2}g^{mn}\hat{\mathbf{q}}^m\hat{\mathbf{k}}^n+\tfrac{1}{2}g^{mn}\hat{\mathbf{q}}^m\hat{\mathbf{k}}^n)$$

$$=-1+\frac{s_R s_L}{2}(-\hat{\mathbf{q}}\cdot\hat{\mathbf{k}}+2\hat{\mathbf{q}}\cdot\hat{\mathbf{k}}-\hat{\mathbf{q}}\cdot\hat{\mathbf{k}})$$

$$=-1 \tag{A19}$$

for both gap and antigap.

For the (particle) gap, the projections (A19) valid for the electric and magnetic terms of the simplified gluon propagator (A7) agree exactly with the projections (A14) and (A16), respectively valid for electric and magnetic terms of the exact form (A1) of the screened perturbative gluon propagator. Furthermore, there is no contribution from the gauge-fixing term; see Eq. (A18). For the antiparticle gaps, the simplified electric contribution (A19) deviates from the exact one (A14). However, as shown by Eq. (A18), the exact result is gauge-fixing-term dependent anyhow, see [19], and moreover subleading.

In summary, the use of the simplified form (A7) of the gluon propagator is justified in weak coupling and to leading logarithm accuracy.

[1] D. Bailin and A. Love, Phys. Rep. **107**, 325 (1984).

[2] M. Alford, K. Rajagopal, and F. Wilczek, Phys. Lett. B **422**, 247 (1998); R. Rapp, T. Schäfer, E.V. Shuryak, and M. Velkovsky, Phys. Rev. Lett. **81**, 53 (1998); T. Schäfer, Nucl. Phys. **A638**, 511C (1998); M. Alford, K. Rajagopal, and F. Wilczek, *ibid.* **A638**, 515C (1998); K. Rajagopal, Suppl. Prog. Theor. Phys. **131**, 619 (1998); J. Berges and K. Rajagopal, Nucl. Phys. **B538**, 215 (1999); M. Alford, K. Rajagopal, and F. Wilczek, *ibid.* **B537**, 443 (1999); T. Schäfer, Nucl. Phys. **A642**, 45 (1998); UKQCD Collaboration, S. Hands and S.E. Morrison, Phys. Rev. D **59**, 116002 (1999); K. Rajagopal, Nucl. Phys. **A642**, 26 (1998); N. Evans, S.D.H. Hsu, and M. Schwetz, Nucl. Phys. **B551**, 275 (1999); UKQCD Collaboration, S. Morrison, Nucl. Phys. B (Proc. Suppl.) **73**, 480 (1999); T. Schäfer and F. Wilczek, Phys. Lett. B **450**, 325 (1999); N. Evans, S.D.H. Hsu, and M. Schwetz, *ibid.* **449**, 281 (1999); R.D. Pisarski and D.H. Rischke, Phys. Rev. Lett. **83**, 37 (1999); K. Langfeld and M. Rho, Nucl. Phys. **A660**, 475 (1999); T. Schäfer and F. Wilczek, Phys. Rev. Lett. **82**, 3956 (1999); D.T. Son, Phys. Rev. D **59**, 094019 (1999); A. Chodos, H. Minakata, and F. Cooper, Phys. Lett. B **449**, 260 (1999); J. Hosek, hep-ph/9812515; G.W. Carter and D. Diakonov, Phys. Rev. D **60**, 016004 (1999); D.K. Hong, Phys. Lett. B **473**, 118 (2000); S. Hands and S. Morrison, hep-lat/9902011; N.O. Agasian, B.O. Kerbikov, and V.I. Shevchenko, Phys. Rep. **320**, 131 (1999); R.D. Pisarski and D.H. Rischke, Phys. Rev. D **60**, 094013 (1999); T.M. Schwarz, S.P. Klevansky, and G. Papp, Phys. Rev. C **60**, 055205 (1999); M. Alford, J. Berges, and K. Rajagopal, Nucl. Phys. **B558**, 219 (1999); T. Schäfer and F. Wilczek, Phys. Rev. D **60**, 074014 (1999); R. Rapp, T. Schäfer, E.V. Shuryak, and M. Velkovsky, hep-ph/9904353; D. Blaschke, D.M. Sedrakian, and K.M. Shahabasian,

astro-ph/9904395; S. Hands and S. Morrison, hep-lat/9905021; G.W. Carter and D. Diakonov, hep-ph/9905465; E. Shuster and D.T. Son, hep-ph/9905448; A. Chodos, F. Cooper, and H. Minakata, hep-ph/9905521; D.K. Hong, hep-ph/9905523; R.D. Pisarski and D.H. Rischke, nucl-th/9906050; D.K. Hong, V.A. Miransky, I.A. Shovkovy, and L.C. Wijewardhana, Phys. Rev. D **61**, 056001 (2000); T. Schäfer and F. Wilczek, *ibid.* **60**, 114033 (1999); D.K. Hong, M. Rho, and I. Zahed, Phys. Lett. B **468**, 261 (1999); M. Rho, nucl-th/9908015; R. Casalbuoni and R. Gatto, Phys. Lett. B **464**, 111 (1999); M. Alford, J. Berges, and K. Rajagopal, Phys. Rev. Lett. **84**, 598 (2000); W.E. Brown, J.T. Liu, and H. Ren, Phys. Rev. D **61**, 114012 (2000); E.V. Shuryak, hep-ph/9908290; S.D.H. Hsu and M. Schwetz, hep-ph/9908310; G.W. Carter and D. Diakonov, Nucl. Phys. **A661**, 62 (1999); D. Blaschke, T. Klahn, and D.N. Voskresensky, astro-ph/9908334; F. Wilczek, hep-ph/9908480; T. Schäfer, Nucl. Phys. **A661**, 621 (1999); A. Chodos, F. Cooper, W. Mao, H. Minakata and A. Singh, Phys. Rev. D **61**, 045011 (2000); R. Casalbuoni and R. Gatto, Phys. Lett. B **469**, 213 (1999); T. Schäfer, hep-ph/9909574; P.F. Bedaque, hep-ph/9910247; M. Alford, J. Berges, and K. Rajagopal, hep-ph/9910254; B. Vanderheyden and A.D. Jackson, Phys. Rev. D **61**, 076004 (2000); N. Evans, J. Hormuzdiar, S.D.H. Hsu, and M. Schwetz, hep-ph/9910313.

[3] A.W. Overhauser, Adv. Phys. **27**, 343 (1978).

[4] D.V. Deryagin, D.Y. Grigorev, and V.A. Rubakov, Int. J. Mod. Phys. A **7**, 659 (1992).

[5] E. Shuster and D.T. Son, hep-ph/9905448.

[6] J. Schwinger, Phys. Rev. **128**, 2425 (1962).

[7] W. Fischler, J. Kogut, and L. Susskind, Phys. Rev. D **19**, 1188 (1979).

[8] H.R. Christiansen and F.A. Schaposnik, Phys. Rev. D **53**, 3260 (1996); **55**, 4920 (1997).

[9] Y.C. Kao and Y.W. Lee, Phys. Rev. D **50**, 1165 (1994).

[10] I. Klebanov, Nucl. Phys. **B262**, 133 (1985); L. Castillejo, P.S. Jones, A.D. Jackson, J.J. Verbaarschot, and A. Jackson, Nucl. Phys. **A501**, 801 (1989); H. Forkel, A.D. Jackson, M. Rho, C. Weiss, A. Wirzba, and H. Bang, *ibid.* **A504**, 818 (1989).

[11] A.S. Goldhaber and N.S. Manton, Phys. Lett. B **198**, 231 (1987); N.S. Manton and P.M. Sutcliffe, *ibid.* **342**, 196 (1995).

[12] T.D. Cohen, Nucl. Phys. **A495**, 545 (1989).

[13] M.A. Nowak, M. Rho, and I. Zahed, *Chiral Nuclear Dynamics* (World Scientific, Singapore, 1996).

[14] M. Rho, A. Wirzba, and I. Zahed (in preparation).

[15] M. Le Bellac, *Thermal Field Theory* (Cambridge University Press, Cambridge, England, 1996).

[16] I. Zahed and D. Zwanziger, Phys. Rev. D **61**, 037501 (2000).

[17] R.T. Cahill and S.M. Gunner, Fiz. B **7**, 171 (1998).

[18] R.D. Pisarski and D.H. Rischke, Phys. Rev. D **61**, 051501 (2000).

[19] T. Schäfer and F. Wilczek, Phys. Rev. D **60**, 114033 (1999).

[20] D.T. Son, Phys. Rev. D **59**, 094019 (1999).

[21] T. Schäfer, hep-ph/9909574.

[22] V.N. Pervushin and D. Ebert, Teor. Mat. Fiz. **36**, 313 (1978); D. Ebert and L. Kaschluhn, Nucl. Phys. **B355**, 123 (1991).

[23] K. Langfeld and M. Rho, Nucl. Phys. **A660**, 475 (1999).

[24] R.D. Pisarski and D.H. Rischke, nucl-th/9907094.

[25] B.-Y. Park, M. Rho, A. Wirzba, and I. Zahed (in preparation).

[26] G. 't Hooft, Nucl. Phys. **B72**, 461 (1974); **B75**, 461 (1974).

[27] D.I. Diakonov and V.Y. Petrov, Nucl. Phys. **B245**, 259 (1984).

[28] D.B. Kaplan, Phys. Lett. B **235**, 163 (1990); Nucl. Phys. **B351**, 137 (1991).